

# NGC 7538 S - a High-Mass Protostar with a Massive Rotating Disk

Göran Sandell<sup>1</sup>, Melvyn Wright<sup>2</sup>, James R. Forster<sup>2</sup>

gsandell@mail.arc.nasa.gov

## ABSTRACT

We report the detection of a massive rotating disk around the high-mass Class 0 candidate NGC 7538 S. The disk is well-resolved with BIMA ( $\theta_A = 3''.7$ ) in 3.4 mm continuum and in H<sup>13</sup>CN J=1→0. It is seen nearly edge on and has a size of  $\sim 30,000$  AU. A young, powerful outflow perpendicular to the rotating disk is mapped in SiO J=2→1 and HCO<sup>+</sup> J=1→0. The dynamical age of the outflow is  $\leq 10,000$  yr. The velocity gradient seen in H<sup>13</sup>CN is consistent with Keplerian rotation. Assuming that the gas is gravitationally bound, the mass of the central object is  $\sim 40 M_\odot$ . The mass of the continuum “disk” is  $\geq 100 M_\odot$  and has a luminosity of  $\sim 10^4 L_\odot$ . H<sup>13</sup>CN gives a mass  $\sim 400 M_\odot$  for the rotating disk, and  $\sim 1000 M_\odot$  for the extended (20'') envelope. Our observations confirm that this is an extremely massive protostar in its earliest stages.

*Subject headings:* ISM: clouds – (stars:) circumstellar matter – stars: formation – stars: pre-main sequence – submillimeter

## 1. Introduction

The formation of high mass stars is still poorly understood, although one expects a high mass protostar to form an accretion disk and drive an outflow similar to what one sees in low mass protostars. Recent surveys show that outflows are very common in high-mass star forming regions (Beuther et al. 2002, and references therein) but that accretion disks have been far more elusive, even though they will have to be larger and have larger velocity

---

<sup>1</sup>Universities Space Research Association, NASA Ames Research Center, MS 144-2, Moffett Field, CA 94035, U.S.A.

<sup>2</sup>Radio Astronomy Laboratory, University of California, Berkeley 601 Campbell Hall, Berkeley, CA 94720, U.S.A.

gradients than accretion disks around low mass stars, which show velocity gradients of only a few tenths of  $\text{km s}^{-1}$ , see e.g. Mannings and Sargent (1997). Although there have been a number of papers reporting rotating disks around high-mass stars, most of these show marginal, barely resolved systems. The best case to date, the young high-mass star IRAS 20126+4104 (Zhang et al. 1998; Cesaroni et al. 1997), has a bolometric luminosity of  $1.3 \cdot 10^4 L_{\odot}$  and drives a massive molecular outflow.

In this letter we present the first results from high spatial resolution BIMA observations of NGC 7538 S. Sandell and Sievers (2003) showed that NGC 7538 S is a cold, very massive elliptical dust source ( $\sim 400 M_{\odot}$ ) associated with  $\text{H}_2\text{O}$  and OH maser emission but only weak free-free emission, which has all the characteristics of a high-mass Class 0 source. The protostellar source is located in the molecular cloud south-east of the large H II region NGC 7538, which is known to contain several centers of active and on-going high-mass star formation (Werner et al. 1979). The distance to NGC 7538 is assumed to be 2.8 kpc. NGC 7538 S is about  $80''$  to the south of the well studied ultracompact H II region IRS 1.

NGC 7538 S is more isolated than IRS 1 and therefore easier to study. We confirm that NGC 7538 S is a high mass protostar and resolve the disk around the protostar both in continuum and in molecular lines. In this letter we present data that suggest that the protostar is surrounded by a massive, rotating accretion disk, which drives a very young and powerful outflow perpendicular to the disk.

## 2. Observations and Data Reduction

The observations of NGC 7538 S were made with the BIMA array in 2001/2002 using two frequency settings in the B and C-array configuration. The correlator was split into four 25 MHz bands resulting in a velocity resolution of  $\sim 0.34 \text{ km s}^{-1}$ . In this letter we base most of our discussion on the frequency setting that included  $\text{H}^{13}\text{CN } J=1 \rightarrow 0$ , and  $\text{HCO}^+ J=1 \rightarrow 0$ , which was observed in both B- and C-arrays. The other frequency setting included the molecular transitions  $\text{HN}^{13}\text{C } J=1 \rightarrow 0$ ,  $\text{SiO } v=0 J=2 \rightarrow 1$  and  $\text{H}^{13}\text{CO}^+ J=1 \rightarrow 0$ . Only one C-array track was obtained in this setting. The images therefore have poorer spatial resolution and sensitivity, but are consistent with the deeper images seen in  $\text{H}^{13}\text{CN}$  and  $\text{HCO}^+$ .

The data were reduced and imaged in a standard way using MIRIAD software (Sault, Teuben and Wright 1995). Phase calibration was applied using observations of the quasar 0102+584 at intervals of 30 minutes. The phase calibrator was observed using an 800 MHz bandwidth for 3 min. 3C454.3 was observed for 10 minutes as a bandpass calibration. The

flux density scale was checked from observations of Mars. The uncertainty in the absolute amplitude scale  $\sim 15\%$ , but the relative amplitude of spectral lines within the same receiver tuning is within  $\sim 5\%$ .

The data were imaged with weighting inversely proportional to the variance in order to obtain the best signal to noise ratio. Averaging 4 spectral channels we obtained an RMS noise level of 24 mJy (0.3 K) with a synthesized beam FWHM  $3''.75 \times 3''.59$  and peak sidelobe level of  $-7\%$ . Spectral windows which did not contain any significant spectral line emission were averaged to provide a continuum image with an RMS  $\sim 3$  mJy. The continuum emission was subtracted from the spectral line channels, and the images deconvolved using the CLEAN algorithm.

### 3. The continuum “disk”

The single dish sub-mm continuum maps (Sandell and Sievers 2003) show NGC 7538 S as an elliptical source embedded in a narrow dust filament. With BIMA we filter out the extended cloud emission and detect only the sub-mm source. At 3.4 mm the continuum source is well resolved with a peak on the northeastern side of an extended elliptical source (Fig 1). A two-component Gaussian fit shows that the northeastern peak is an unresolved point-like source with a flux density of 20 mJy offset  $3''.7$ ,  $0''.5$  from the nominal sub-mm position. The position of the 3.4 mm point source coincides with the OH and H<sub>2</sub>O maser and the 6 cm VLA position (Argon, Reid and Menten 2000; Kameya et al. 1990, O. Kameya 2003, private communication). At 6 cm the VLA source has a flux density of 2.8 mJy. If the 6 cm emission is due to an ionized wind, i.e. follows a  $\nu^{0.6}$  frequency dependence, about half of the 3.4 mm flux is an excess, presumably due to hot dust close to the protostar. However, the free-free emission could also have a steeper frequency dependence. In the following we assume that the point-source emission is all due to free-free emission.

The extended elliptical source has a size of  $13''.7 \times 8''.1$  and a position angle (P.A) of  $71^\circ$ , offset  $+1''.7$ ,  $-0''.4$  from the nominal sub-mm position with an integrated flux density of 190 mJy, i.e. it agrees within errors both in size and position with the sub-millimeter source. In this respect this source differs from IRS 1 and IRS 9, which both appear unresolved at 3 mm (van der Tak et al. 2000) and from nearby low mass protostars, which are only marginally resolved with a  $\sim 0''.5$  beam (Looney, Mundy and Welch 2000).

To estimate a mass from our continuum observations we adopt a single-temperature optically thin thermal dust model. The total mass of gas and dust, M, can then be expressed as  $M = S_\nu D^2 / (\kappa_\nu B_\nu(T_d))$ , where  $B_\nu(T_d)$  is the Planck function,  $\kappa_\nu$  is the dust mass opacity,

$T_d$  is the dust temperature,  $D$  is the distance, and  $S_\nu$  is the integrated flux density at the frequency  $\nu$ . We assume a gas to dust ratio of 100 and adopt a dust mass opacity at 87 GHz,  $\kappa_{87} = 0.0073 \text{ cm}^2 \text{ g}^{-1}$ , corresponding to a dust emissivity,  $\beta = 1$ . This value was also used by Looney, Mundy and Welch (2000) in their BIMA study of low mass protostellar disks. With a dust temperature,  $T_d = 35 \text{ K}$  Sandell and Sievers (2003), we find the total mass of the continuum disk to be  $100 M_\odot$ . We note, however, that the isothermal greybody fits by Sandell and Sievers (2003) predicted a steeper emissivity law,  $\beta = 1.6$ , which would result in a five times smaller mass opacity and hence a more massive disk.

#### 4. A rotating protostellar disk ?

The map of integrated  $\text{H}^{13}\text{CN } J=1 \rightarrow 0$  emission (Fig. 1) shows a bright elongated source surrounded by a more extended envelope superposed on the 3.4 mm continuum. The elongated source in the center of the map has the same orientation and extent as the source we see in dust continuum. For a two-component Gaussian fit, we find the bright emission offset  $2''.0$ ,  $1''.0$  from the nominal sub-mm position, i.e. within errors coincident with the 6 cm VLA and the OH/ $\text{H}_2\text{O}$  maser position at  $+3''.7$ ,  $+1''.0$ . The fitted size:  $11''.1 \times 6''.8$  with a P.A. =  $55 \pm 5^\circ$ , is slightly smaller than the continuum disk. The position velocity plot taken along the major axis of the bright  $\text{H}^{13}\text{CN}$  emission shows a clear velocity gradient across the source (Fig 2). The emission is red-shifted to the southwest and blue-shifted to the northeast with the center of symmetry coinciding within  $2''$  with the position of the protostar. A rotation curve derived from these data is slightly asymmetric with the central velocity close to  $-56 \text{ km s}^{-1}$ . It reaches a peak of  $\pm 1.35 \text{ km s}^{-1}$  at a radius of  $5''$  (14000 au) in both directions. The observed velocity gradient corresponds to an enclosed mass of  $\sim 30 / \sin^2 i M_\odot$  for a rotating disk to be gravitationally bound. With an assumed inclination,  $i = 60^\circ$  (see below) the mass is  $\sim 40 M_\odot$ .

$\text{H}^{13}\text{CO}^+ J=1 \rightarrow 0$  and  $\text{HN}^{13}\text{C } J=1 \rightarrow 0$  were observed with only one C-array track and therefore lack the spatial resolution to resolve the disk. Both molecules show strong extended emission towards the protostar and we can therefore use all three molecules to get an estimate of the mass of the disk and the surrounding molecular envelope. For estimating column densities and masses we assume LTE and that the excitation temperature for all molecules is the same as that for the dust, i.e. 35 K. The permanent dipole moments are taken from Blake et al. (1987), except for  $\text{HCO}^+$ , for which we adopt  $\mu = 4.07$  Debye (Haese and Woods 1979). For total mass estimates we use abundance ratios to  $\text{H}_2$  similar to those in the OMC-1 extended ridge (Blake et al. 1987), i.e.  $[\text{HCO}^+]/[\text{H}_2] = 2 \cdot 10^{-9}$ ,  $[\text{HCN}]/[\text{H}_2] = 5 \cdot 10^{-9}$ , and  $[\text{HNC}]/[\text{H}_2] = 5 \cdot 10^{-10}$ , and the isotope ratio,  $^{12}\text{C}/^{13}\text{C} = 85$  (Wilson and

Rood 1994). For  $\text{H}^{13}\text{CN}$  we get a peak column density of  $7 \cdot 10^{13} \text{ cm}^{-2}$  for the disk and  $5 \cdot 10^{13} \text{ cm}^{-2}$  for the surrounding envelope, resulting in a disk mass  $\sim 400 M_{\odot}$  and an envelope  $\sim 1000 M_{\odot}$ . For  $\text{H}^{13}\text{CO}^{+}$  and  $\text{HN}^{13}\text{C}$  we do not have enough spatial resolution to separate the disk and the envelope, but we derive combined masses  $\sim 1000$  and  $3000 M_{\odot}$ , for  $\text{H}^{13}\text{CO}^{+}$  and  $\text{HN}^{13}\text{C}$ , respectively.

## 5. The high velocity outflow

We see clear high velocity wings in both  $\text{HCO}^{+} \text{ J}=1 \rightarrow 0$  and  $\text{SiO } v=0 \text{ J}=2 \rightarrow 1$ . Towards the protostar the  $\text{HCO}^{+}$  shows dominantly blue-shifted high velocity emission extending  $29 \text{ km s}^{-1}$  from the systemic velocity ( $\sim -56 \text{ km s}^{-1}$ ) with a sharp, deep absorption on the red-side at nearby cloud velocities, suggesting infall of the surrounding cooler envelope. The  $\text{SiO}$  line wings at the position of the disk appear more symmetric, presumably due to the broader beam and the absence of self-absorption. Both  $\text{SiO}$  and  $\text{HCO}^{+}$  show the same distribution of the high velocity gas. Here we only present the results from our  $\text{HCO}^{+}$  imaging, which has better signal-to-noise and higher spatial resolution.

$\text{HCO}^{+}$  shows a strong, compact, jet-like bipolar high velocity outflow at a pa of  $147^{\circ} \pm 5^{\circ}$  (Fig 3). The symmetry axis of the outflow passes through the VLA source. The  $\text{H}^{13}\text{CN}$  map shows that the surrounding cloud core is more dense to the north than to the south. This is also evident from the outflow, which is much more compact to the northwest than to the southeast. In the northwest the outflow is blue-shifted and terminates sharply at  $\sim 7''$  from the protostar. To the southeast the outflow is mostly red-shifted and well collimated (aspect ratio  $\sim 2:1$ ) to  $\sim 16''$  from the protostar, where it expands to become a more wide angle flow, presumably breaking out of the cloud at  $\sim 30''$  from the protostar. The strongest blue-shifted emission is seen at the tip of the northwestern outflow lobe with outflow velocities extending to  $27 \text{ km s}^{-1}$  from the systemic cloud velocity. The southeastern outflow lobe shows both red- and blue-shifted emission with outflow velocities of  $\sim 24 \text{ km s}^{-1}$  in the red and blue-shifted emission up to  $18 \text{ km s}^{-1}$  in the dense, well collimated part of the outflow. At the tip of the outflow, the outflow velocities are lower, presumably because the high velocity gas is too tenuous to be excited in  $\text{HCO}^{+}$ .

Since there is both blue- and red-shifted emission to the southeast, and little overlap between the outflow lobes at the star, the outflow must have fairly high inclination. In the following we assume an inclination of  $60^{\circ}$ , which is roughly consistent with the observed aspect ratio of the disk, i.e. we see the disk almost edge on. The northwestern blue-shifted outflow lobe is still confined by the surrounding cloud, while the southeast outflow appears to have broken through the dense cloud core. Since the extent of the outflow to the southeast

is less well defined we derive outflow characteristics mainly from the northwest blue-shifted outflow lobe.

The blue-shifted outflow lobe gives a dynamical time scale of  $\sim 2,000$  yr, while the red-shifted emission gives  $\sim 10,000$  yr, corrected for a  $60^\circ$  inclination. Note that the velocities are probably much higher in the red-shifted outflow, since it is expanding through a less dense cloud. We assume  $\text{HCO}^+$  to be optically thin with an excitation temperature of 30 K, the same as Shepherd and Churchwell (1996) used in their study of outflows from high mass stars. If we further assume a normal  $\text{HCO}^+$  abundance in the outflow (Section 4), we find a mass of  $9 M_\odot$  for the northwest blue-shifted outflow and  $8 M_\odot$  for the redshifted gas in the southeast outflow lobe. The mass weighted momentum flux,  $F = mv/t_{\text{dyn}}$  and the mechanical luminosity,  $L_{\text{mec}} = mv^3/2r$ , where  $r$  is the extent of the outflow, is  $90 \cdot 10^{-3} M_\odot \text{kms}^{-1} \text{yr}^{-1}$ , and  $130 L_\odot$  for the blue outflow alone. The mass loss rate, based only on the confined blue-shifted outflow, could be as high as  $\sim 5 \cdot 10^{-3} M_\odot \text{yr}^{-1}$ .

## 6. Discussion and Conclusions

The new data we present in our letter reveal a well resolved elliptical source mapped in several optically thin lines as well as in 3.4 mm continuum. The peak of the line emission is centered within  $1'' - 2''$  of the VLA 6cm continuum, OH, and  $\text{H}_2\text{O}$  maser emission position. The 3.4 mm continuum emission has an extent similar to the elongated source seen in optically thin high-density tracers with a peak (hotspot) within  $1''$  of the VLA and maser position. Follow-up observations at 1 mm in both line and continuum (Sandell, Wright, & Forster 2003, in preparation) show the disk more clearly and show that  $\text{CH}_3\text{CN J}=12 \rightarrow 11$ , which traces hot gas, is centered within  $0''.2$  of this position. FIR observations (Werner et al. 1979; Thronson and Harper 1979) show a FIR source with a luminosity of  $\sim 10^4 L_\odot$ , with a narrow FIR spectral energy distribution, strongly suggesting that the FIR luminosity is produced by a single central source. The FIR source has no near or mid-IR counterpart suggesting that it is heavily obscured. The FIR observations do not have enough spatial resolution or positional accuracy to confirm that the luminosity originates from the the OH/ $\text{H}_2\text{O}$  masers, but all 1665 MHz OH masers require a luminous source for their excitation; therefore we conclude that the source powering the OH maser is the origin for the bulk of the observed FIR luminosity.

The  $\text{H}^{13}\text{CN}$  map (Fig 2) shows a clear velocity gradient along the major axis of the elliptical source. If we interpret this as a rotating disk gravitationally bound by the central source, we find that the center of symmetry is within  $\leq 2''$  of the maser source. Since this position also lies on the symmetry axis of the outflow, defined by our high spatial resolution

HCO<sup>+</sup> map, there is no doubt that this is the center of the mass and the protostar. From the observed velocity gradient we derive an enclosed mass of 40 M<sub>⊙</sub> (Section 4). Since we have resolved the emission of the disk from the envelope, we can use the integrated emission of the disk to derive a mass. Assuming normal abundances and a kinetic temperature of 35 K for the disk we find a mass  $\sim 400$  M<sub>⊙</sub> from the H<sup>13</sup>CN, and  $\sim 100$  M<sub>⊙</sub> from the 3.4 mm continuum emission. Considering the uncertainties in molecular abundances and dust opacity, these estimates are in reasonable agreement. The mass of the central object and the disk are of the same magnitude.

The bipolar HCO<sup>+</sup> high velocity outflow (Section 5) may be driven by the rotating protostellar disk. The outflow is extremely young; the dynamical timescale from the blue-shifted outflow indicates an age of  $\leq 2000$  yr, with an upper limit of 10,000 yr derived from the red-shifted outflow. Shepherd and Churchwell (1996) show that there is a clear correlation between mass loss rate and bolometric luminosity of the central source over a wide range of luminosities. If we use the correlation derived by Shepherd and Churchwell (1996), our observed mass loss rate corresponds to a luminosity of close to  $10^5$  L<sub>⊙</sub>, while the observed luminosity is only  $10^4$  L<sub>⊙</sub>. Our observations therefore suggest an elevated mass loss rate in the very earliest stages of the formation of a massive star. Since we find the rotating accretion disk to be more massive than the central protostar, the disk will be highly unstable and is likely to feed both the outflow and the central accreting protostar. Model calculations by Yorke, Bodenheimer and Laughlin (1995) for a somewhat less massive central star (10 M<sub>⊙</sub>), find that the accretion disk evolves into a thin flared disk with a ratio of  $M_{\star}/M_{disk} \sim 4$ , for all the models that they computed. Even though they ignored magnetic fields, these models should still give an idea of how the disk is expected to evolve.

There is only one near-IR source in the vicinity of NGC 7538 S, IRS 11 (Fig 3). This IR source is associated with nebulosity and a knot of vibrationally excited H<sub>2</sub> emission, suggesting that it is most likely a young star. There are several additional H<sub>2</sub> knots in the vicinity of NGC 7538 S; two appear to be associated with the molecular outflow. The only other evidence for young objects in this region is an unexplained high velocity HCO<sup>+</sup> emission feature 10'' southwest of the protostar, three vibrationally excited H<sub>2</sub> knots  $\sim 20''$  east of it, and an H<sub>2</sub>O maser  $\sim 30''$  west of it. The high velocity HCO<sup>+</sup> could be part of a wide angle disk-wind or due to a young low luminosity source in the outskirts of the disk. This could explain the observed asymmetry in the continuum disk (more extended to the southwest), but it cannot produce the observed velocity gradient. The eastern H<sub>2</sub> knots and the western H<sub>2</sub>O maser are unrelated to the protostellar source.

It is therefore possible that the extended disk/envelope system harbours yet another protostar. Such a protostar would have much lower luminosity and mass, since the massive

protostar can explain most, if not all of the observed luminosity. Although high-mass stars usually form in clusters, all the evidence we have so far, suggest that NGC 7538 S is an isolated high mass star. If the central protostar is a single star, it may evolve into a late O or early B-star.

We thank Dr. Osamu Kameya for sharing his unpublished VLA results with us. The BIMA array is operated by the Universities of California (Berkeley), Illinois, and Maryland with support from the National Science Foundation.

## REFERENCES

- Argon, A. L., Reid, M. J., and Menten, K. M. 2000, *ApJS*, 129, 159
- Beuther, H., Schilke, P., Menten, K. M., Motte, F., M., Shridharan, T. K., and Wyrowski, F. 2002, *ApJ*, 566, 945
- Blake, G. A., Sutton, E. C., Masson, C. R., Phillips, T. G. 1987, *ApJ*, 315, 621
- Cesaroni, R., Felli, M., Testi, L., Walmsley, C. M., and Olmi, L. 1997, *A&A*, 325, 725
- Davis, C.J., Moriarty-Schieven, G., Eisloffel, J., Hoare, M. G., and Ray, T.P. 1998, *AJ*, 115, 1118
- Haese, N. N., Woods, R. C. 1979, *Chem. Phys. Lett.*, 61, 396
- Kameya, O., Morita, K. -I., T.I., Kawabe, R., and Ishiguro, M. 1989, *ApJ*, 355, 562
- Looney, L. W., Mundy, L. G., and Welch, W.J. 2000, *ApJ*, 529, 477
- Mannings, V., and Sargent, A. 1997, *ApJ*, 490, 792
- Sandell, G., and Sievers, A. 2003, *ApJ*, submitted
- Sault, R. J., Teuben, P. J., and Wright, M. C. H., 1995, in *ASP Conf. Ser. 77: Astronomical Data Analysis Software and Systems IV*, Eds. R.A. Shaw, H.E. Payne, and J.J.E. Hayes (Astronomical Society of the Pacific: San Francisco), p. 433
- Shepherd, D. S., and Churchwell, E. 1996, *ApJ*, 472, 225
- van der Tak, F. F. S., van Dishoeck, E. F., Evans II, N. J., and Blake, G. A. 2000, *ApJ*, 537



Werner, M. W., Becklin, E. E., Gatley, I., Matthews, K., Neugebauer, G., and Wynn-Williams, C.G. 1979, MNRAS, 188, 463

Thronson, H. A., Jr, and Harper, D. A. 1979, ApJ, 230, 133

Wilson, T. L., and Rood, R. T. 1994, ARA&A, 32, 192

Yorke, H. W., Bodenheimer, P., and Laughlin, G. 1995, ApJ, 443, 199

Zhang, Q., Hunter, T. R., and Sridharan, T. K. 1998, ApJ, 505, L151

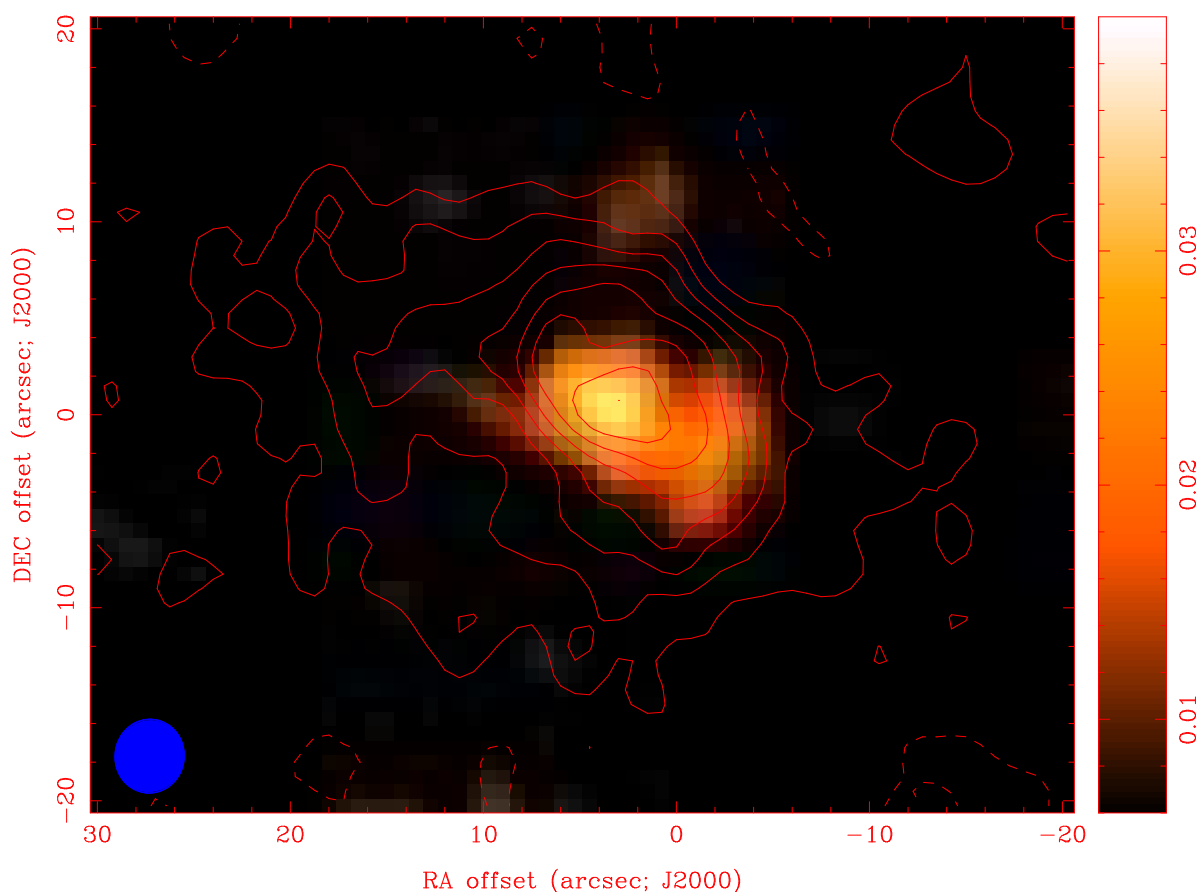


Fig. 1.— Color image of 3.4 mm continuum emission of NGC 7538 S overlaid with contours of H<sup>13</sup>CN J=1→0 emission integrated over the velocity range  $-70$  to  $-40$  km s<sup>-1</sup>. The maps

are offset  $(-3''.7, -0''.5)$  from the 3.4 mm peak:  $\alpha(2000.0) = 23^h 13^m 44^s.98$ ,  $\delta(2000.0) = +61^\circ 26' 49''.2$ . The intensity scale for the continuum is in  $\text{Jy beam}^{-1}$ . The contours for the  $\text{H}^{13}\text{CN}$  emission go from  $-6 \text{ K km s}^{-1}$  (dotted contours) and thereafter from  $6 \text{ K km s}^{-1}$  with steps of  $6 \text{ K km s}^{-1}$ . The beam FWHM is plotted in blue.

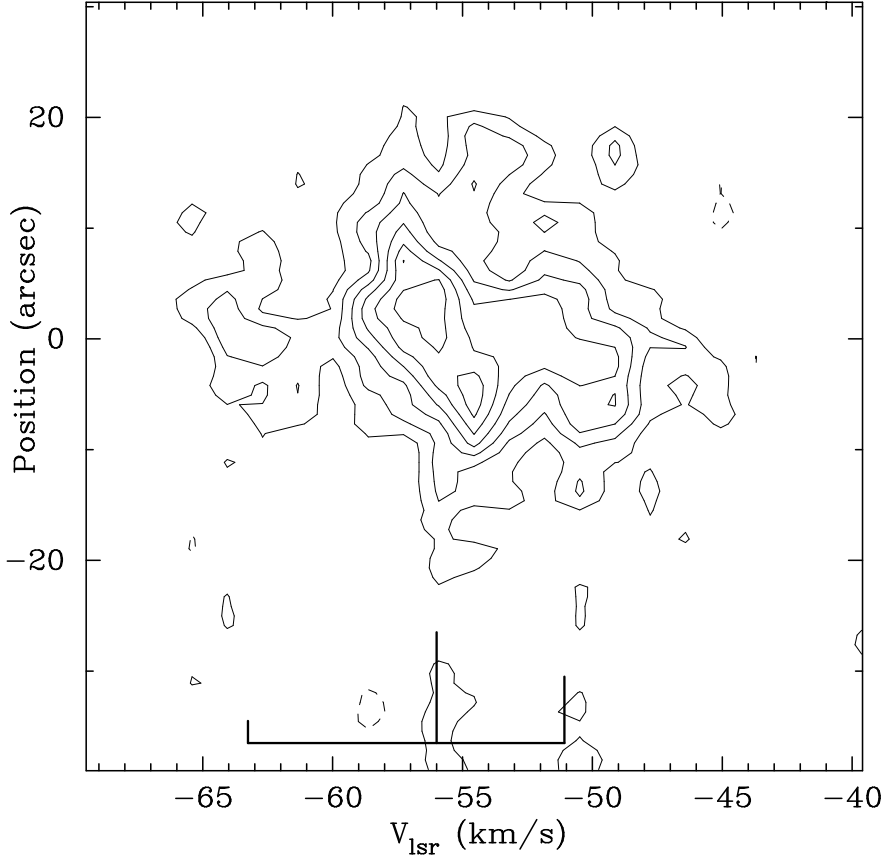


Fig. 2.— Position velocity plot of the  $\text{H}^{13}\text{CN}$   $J=1 \rightarrow 0$  emission along the disk plane at  $pa = 60.0^\circ$ . Positive offsets are to the northeast. The velocity gradient is seen in all three hyperfine lines. The velocity scale is relative to the strongest hyperfine component,  $F = 2 - 1$ , centered at a systemic velocity of  $\sim -56 \text{ km s}^{-1}$ . The line drawing at the bottom of the plot shows the position of three hyperfine components and their relative intensity. The disk emission is red-shifted to the southwest and blue-shifted to the northeast (see text).

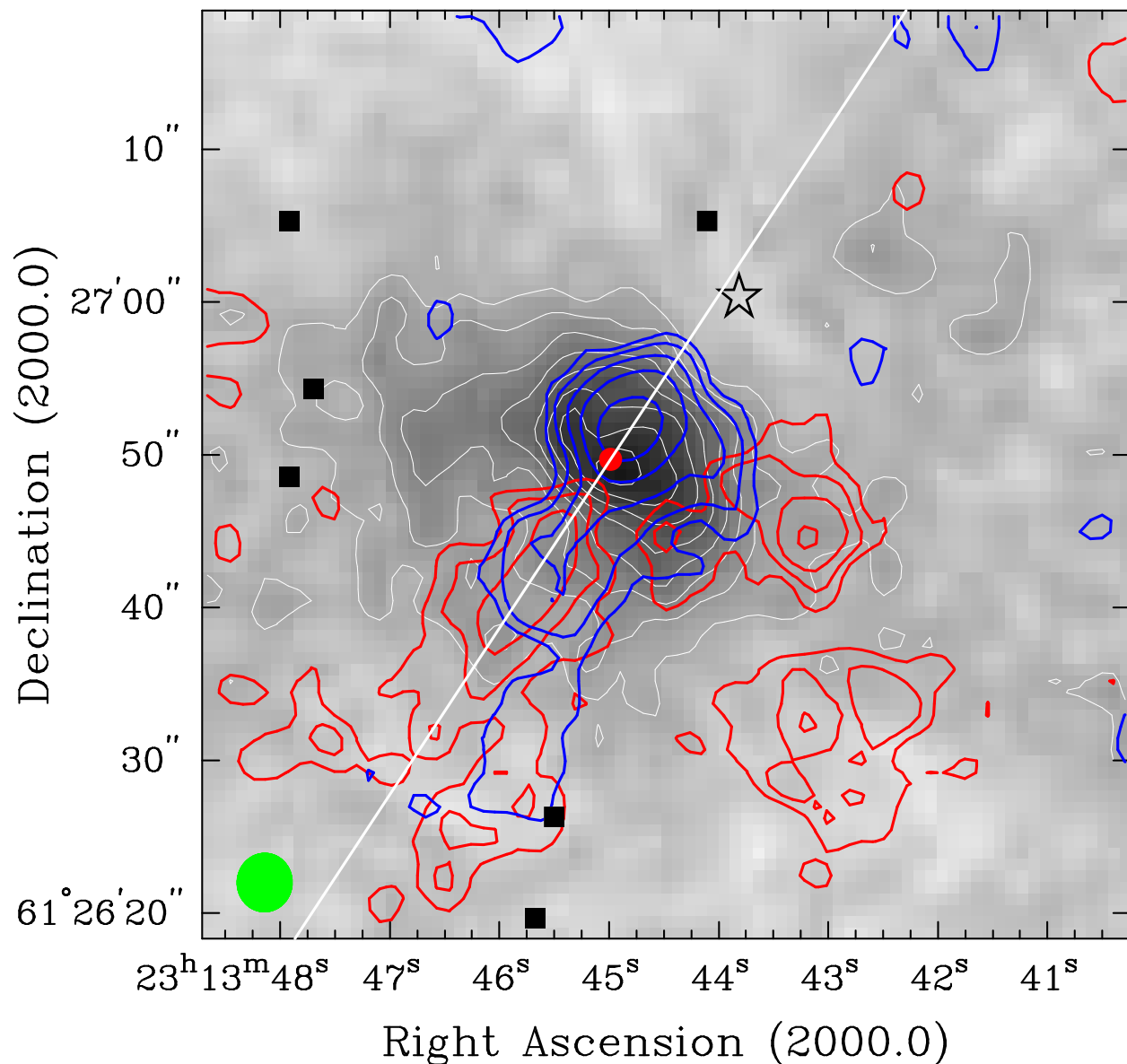


Fig. 3.— Contour map of blue- and red-shifted high velocity HCO<sup>+</sup> J=1→0 integrated over 20 km s<sup>-1</sup> overlaid on a greyscale image of integrated H<sup>13</sup>CN. The red circle marks the position of the protostar and the white line shows the symmetry axis of the outflow. The star symbol marks the position of IRS 11 and the filled squares are H<sub>2</sub> knots from Davis et al. (1998). The contours are logarithmic and start at 4.6 K km s<sup>-1</sup> for HCO<sup>+</sup> with a step of 10<sup>0.2N</sup>, where N= 1,2.. The beam FWHM is plotted in green.